Article no. 21

THE CIVIL ENGINEERING JOURNAL 2-2018

NUMERICAL SIMULATION OF STRESS WAVE PROPAGATION IN SAP CONCRETE

Zhenqun Sang[1,2], Zhiping Deng[1,3], Jianglin Xi[4], Huibin Yao[2], Jiang Wu[2]*

1. *Army Logistics University of PLA, Chongqing, 401311, China; dzpcorner@163.com*
2. *Communication Institute for NICOs, Army Engineering University of PLA, Chongqing, 400035, China;*
3. *Technology Brigade of Aerospace Engineering, Beijing, 100192, China;*
4. *Army Engineering University of PLA, Nanjing, 210007, China.*

ABSTRACT

The SAP (Super Absorbent Polymers) concrete is a new kind of concrete materials with uniformly distributed spherical pores with diameter of millimetre-size. The study on propagation characteristics of SAP concrete is important to give a full comprehending of its dynamic mechanical properties.Based on the ABAQUS platform, the numerical model to simulate the propagation of stress wave in SAP concrete was established by introducing the function of dynamic compressive strength increment DIF-$f_{c,r}$ caused by strain-rate effect of the material itself and strain rate into the expanded Drucker-Prager model. Totally six kinds of triangle stress wave have been investigated, and the transmitted stress wave for each triangle incident stress wave through different pressure bars has been analysed. Based on the numerical calculation, the laws of attenuation and dispersion effect on stress waves in the SAP concrete with evenly distributed millimetre-size spherical pores inside have been analysed.

KEYWORDS

SAP concrete, Stress wave propagation, Strain-rate effect, SHPB test, Attenuation and dispersion effect

INTRODUCTION

SAP (Super Absorbent Polymers) concrete is a kind of porous material with spherical millimetre-size pores inside the concrete [1-3]. The average diameter of the saturated SAP is 5mm. In the process of curing, the spherical saturated SAP beads can slowly dehydrate and separate from the cement paste after shrinkage, and eventually leave closed millimetre-size pores evenly distributed in the concrete. SAP concrete have been used in the island far from the mainland, which can substitute the normal coarse aggregate with saturated SAP and reduce the cost by transportation of the normal aggregate. The stress wave propagation characteristic is an important part of the study of the dynamic mechanical properties, and it is also a basic issue in protective engineering application needs to be proved. When the propagation of stress waves in the medium cause plastic deformation of the material, the original elastic stress wave becomes the plastic stress wave. For plastic stress wave, the wave velocity is determined by two parts: one is the density of dielectric material; the second part is the tangent modulus $d\sigma/d\varepsilon$ of the plastic part on the stress-strain curve of dielectric materials under dynamic loading. For hardening decreasing material, the tangent modulus of stress-strain curve decreases with the increase of strain. Thus, the wave velocity of plastic stress decreases with increase of stress. The wave profile is becoming

more and more flat and finally the wave dispersion appears which is also called the constitutive dispersion [4].

In the case of the hardening increasing material, the elastic-plastic stress wave will become steeper and steeper in the propagation process, and then the shock wave will be formed. For linearly hardened materials, the wave front remains unchanged during propagation. Usually, tangent modulus of the plastic parts of stress-strain curve for a certain material is smaller than elastic modulus, which will cause the propagation speed of plastic stress wave is slower than elastic stress wave, thus the phenomenon of chasing after unloading will appear. When there is interface, the steep wave front will change to form multiple steps due to the reflection of plastic stress wave on the interface and unloading effect of the elastic unloading stress wave. The time history curve of stress pulse appears obvious waveform dispersion phenomenon due to the stepped wave front, and this kind of wave dispersion is different to constitutive dispersion, which is called interface dispersion [5-7].

The SAP concrete has the spatial reticulated shell structures, in which there is much free shell surface and three-dimensional distribution of internal stress. There is complex reflection effect for the tress wave propagating between the free surface inside the concrete. Furthermore, the constitutive model of the SAP concrete exhibits nonlinear properties such as plastic characteristics in whole or partial part of the material. [8-9]. So, it is difficult to theoretically conduct an analytical analysis, especially when partial or whole plastic formation appears and it will be more complex than the elastic stress wave to analyse the reflection effect on the interface for plastic stress wave. Therefore, it is difficult to resolve the propagation behaviour of stress wave in the SAP concrete, and it is necessary to carry out the research through the numerical method of finite element. In this paper, the expanded Drucker-Prager model [10-11] has been used with further introduction of the strain rate effect of the mortar matrix to study the stress wave propagation characteristics in SAP concrete.

THE ESTABLISHMENT OF THE NUMERICAL MODEL

Simplification of the SHPB test equipment

The simplified SHPB (Split Hopkinson Pressure Bar) experiment device has been used to study the stress wave propagation characteristics in SAP concrete. The simplified calculation model of SHPB experiment device mainly includes the loading stress wave, specimen, incident bar and transmitted bar with uniform cross-section, as shown in Figure 1.

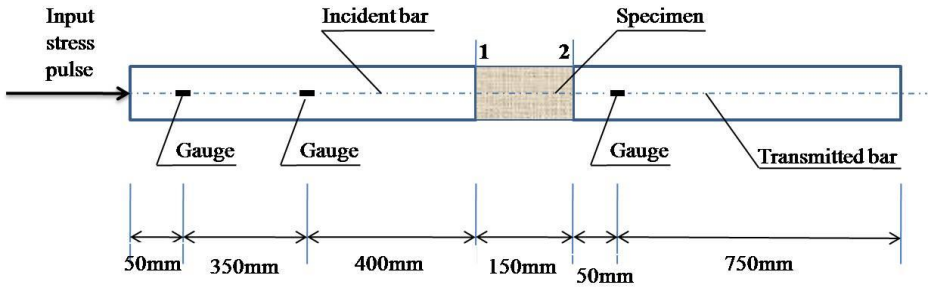

Fig. 1 – Schematic diagram of the numerical simulation for prorogation of stress wave

The circular cross-section of specimen and pressure bars is simplified to square cross - section. The material model for incident bar and transmitted bar used in the simulation is a linear elastic model. The friction coefficient between the surface of pressure bar and specimen is 0,

which means the friction effect of the interface is ignored in the calculation. The incident bar and transmitted bar are mainly to load and record the stress wave propagation through the specimen. It is necessary to have a long specimen, thus, a complete stress wave with at least a wave length will exist in the specimen. The length of specimen is set to be 150mm with comprehensive regarding of the complete stress wave propagating in the specimen and calculation cost.

Constitutive model of the mortar matrix

The numerical research conducted in this paper is mainly based on the experimental data of SHPB test of the SAP concrete with different porosities, which is 10%, 20%, 30% and 40% respectively, and under quasi static loading or dynamic loading with three strain rate levels of 70/s, 100/s and 140/s. The corresponding mechanical performance data of the SAP concrete is shown in Table 1.The uniaxial compressive stress-strain curve under quasi static loading of the mortar matrix is shown in Figure 2 (a), and this typical stress-strain curve can be simplified as shown in Figure 2 (b). In the generic numerical simulation software ABAQUS, the expanded Drucker-Prager model can describe the characteristics of the stress-strain relationship shown in Figure 2, and the expanded Drucker - Prager model can also reflect the hydrostatic pressure correlation of the materials.

Tab. 1 - Mechanical properties of SAP concrete subjected to quasi static and high strain-rate loading

Theoretical porosity (%)	Real porosity (%)	Quasi static strength (MPa)	Average strain rate (/s)	Compressive strength (MPa)	DIF-f_c
			79.7	95.4	1.78
10	9.5	53.6	107.6	102.4	1.91
			140.2	108.8	2.03
			68.2	68.2	1.80
20	19.3	37.9	100.0	74.7	1.97
			126.9	80.3	2.12
			70.5	40.1	1.92
30	27.8	20.9	104.7	45.1	2.16
			142.7	50.8	2.43
			72.1	30.7	1.97
40	38.7	15.6	101.5	36.0	2.31
			141.5	40.2	2.58

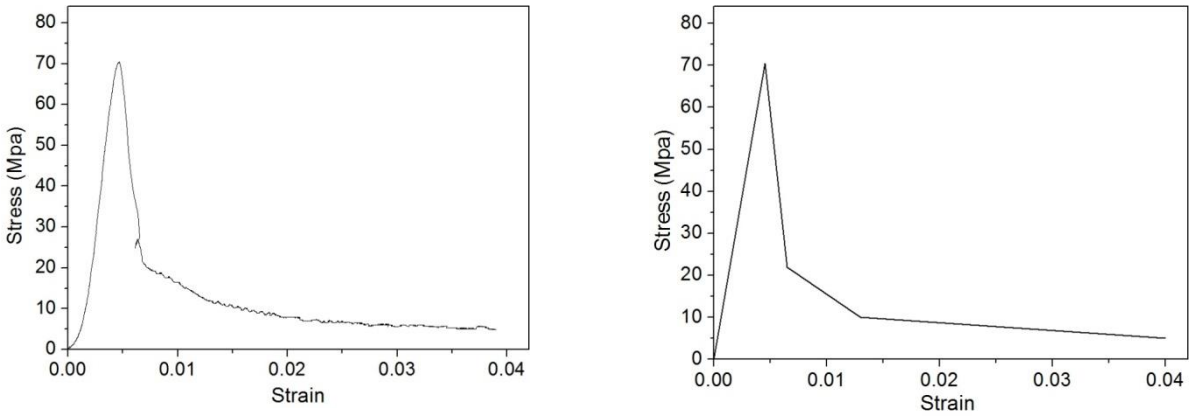

(a) Quasi-static uniaxial stress-strain curve of the mortar matrix *(b) Simplified quasi-static uniaxial stress-strain curve of the mortar matrix*

Fig. 2 – Quasi-static uniaxial stress-strain curve

The pressure bar used in the numerical model includes three different kinds of materials: mortar matrix of SAP concrete, steel fiber concrete, and corundum concrete. The pressure bar of mortar matrix of SAP concrete is mainly used to study the waveform changes before and after the SAP concrete specimens. The pressure bar of steel fiber concrete and corundum concrete mainly used in protective engineering is to study the influence of multilayer material with SAP concrete middle layer on stress wave propagation. When the material of pressure and specimen are the same, the wave impedance of pressure bar and specimen is equal and it can reduce the reflection of stress wave on the interface, at the same time decrease the stress wave attenuation and dispersion in the pressure bar. The linear elastic model was selected for pressure bar and the density, elastic modulus and Poisson's ratio were in accordance with the mortar matrix. When pressure bar using steel fiber concrete and corundum concrete, the material model was also the same linear elastic model, material density and elastic modulus obtained from the research before. For the convenience of description, the pressure of mortar matrix, steel fiber reinforced concrete and corundum aggregate concrete were named pressure bar 1, pressure bar 2 and pressure bar 3 respectively. From the pressure bar 1 to 3, the impedance between pressure bar and SAP concrete specimen increases. The expanded Drucker - Prager model was used to describe the SAP concrete specimen, and the model parameters are listed in Table 2.

Tab. 2 - Material properties involved in the numerical model

Material	density (kg/m^3)	Elastic modulus (GPa)	Poisson's ratio	Compressive strength (MPa)	Friction angle β	Dilatancy angle ψ	K
Pressure bar 1	2172	24.2	0.21	—	—	—	—
Pressure bar 2	2700	47.5	0.18	—	—	—	—
Pressure bar 3	3800	400	0.3	—	—	—	—
Mortar matrix	2172	24.2	0.21	70.5	46°	46°	1

The parameters for expanded Drucker - Prager model displayed in Table 2 do not consider the strain rate effect of SAP concrete material itself, which needs to be added to the expanded Drucker - Prager model. The strain rate effect of SAP concrete material itself can be obtained by numerical studying the lateral inertial confinement effect and friction effect in SHPB test of the SAP concrete with different porosities. The formula suggested by CEB [12] can be used to fit the function of the strain rate effect caused by material itself and strain rate, by which the fitting parameters *β* and *γ* can be obtained for each porosity. Then, the function of parameter *β* and *γ* and porosity can be fitted as:

$$\beta = \frac{0.5804}{1+e^{1.625-0.0568V}} \tag{1}$$

$$\gamma = 1.69\times10^{-4}V^2 - 0.0134V + 0.2684 \tag{2}$$

According to the fitting Equation 1 and Equation 2, it can be deduced that parameters *β*=0.095, *γ*=0.268 when the porosity is equal to zero, namely this parameter value of *β* and *γ* represent the strain rate effect at high strain rates of mortar matrix caused by the material itself. Thus, the variation of dynamic compressive strength increment caused by materials itself of the mortar matrix and strain rate can be obtained as the equation recommended by CEB:

$$DIF - f_c = \frac{f_c}{f_{cs}} = \begin{cases} (\dot{\varepsilon}/\dot{\varepsilon}_s)^{1.026\alpha_s} & \dot{\varepsilon} \le 30/s \\ 0.268(\dot{\varepsilon}/\dot{\varepsilon}_s)^{0.095} & \dot{\varepsilon} \ge 30/s \end{cases} \tag{3}$$

The dynamic mechanical behaviour of SAP concrete can be simulated by introduction of the Equation 3 into expanded Drucker - Prager model. However, the Equation 3 may contain some errors coming from the experiment, data processing and numerical model. The strain rate effect parameters *β* and *γ*=0.268 for mortar matrix need to be adjusted, based on the stress-strain curves in SHPB test, through trial calculation in order to accurately obtain the stress wave propagation law for SAP concrete with different porosities. The strain rate effect parameters *β* and *γ*=0.268 for mortar matrix after calibration are shown in Table 3.

Tab. 3 - Parameter β and γ of the matrix

Porosity of the specimen (%)	*β*	*γ*
10	1.03	2.38
20	1.12	2.22
30	1.19	2.13
40	1.25	1.97

Incident stress wave

The incident stress wave is a triangle wave with the pulse time 40μsor 80μs, the peak stress 5MPa, 15MPa or 25MPa.The six kinds of incident stress waves are shown in Figure 3. For convenience, the pulse time of incident stress wave is represented by "T" and the peak stress by "F", namely the "$T_{40}F_{15}$" indicates the incident stress wave with pulse time 40μsand peak stress 15MPa.

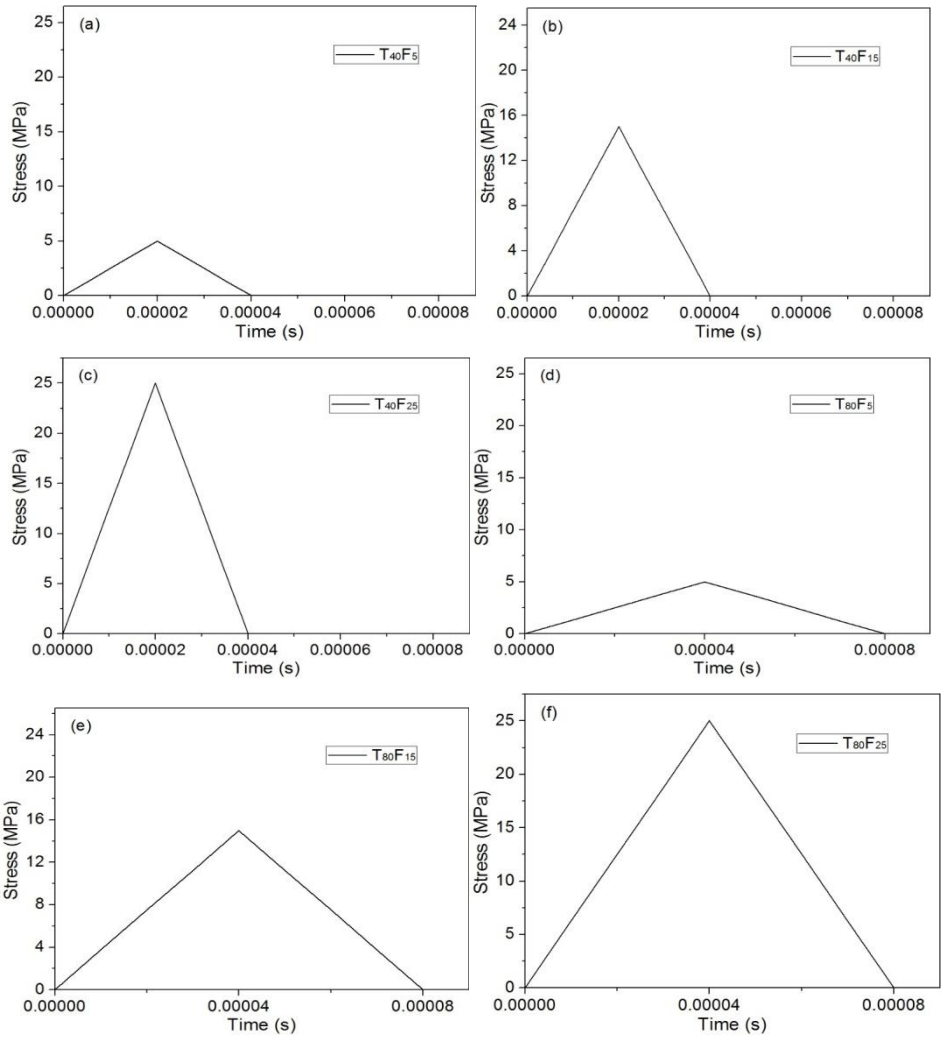

Fig. 3 – Incident stress pulse

Mesh generation

To improve the mesh quality for dynamic calculation, the cross - section shape of the pressure bar and specimen should be simplified: 1) for the pressure bar, the circular cross - section was simplified to square cross - section with original cross - section area, length and volume; 2) the cylinder specimen was simplified to rectangular shape with the same thickness and volume. Trial calculation indicated that the mesh quality around the pores was the main factor that influences the precision of dynamic calculation. To avoid hourglass during calculation, the mesh quality must be guaranteed strictly. The structured mesh technology has been and C3D8R (eight nodes three-

dimensional stress reduced integral unit) have been adopted to mesh the incident bar, transmitted bar and specimens. Based on symmetry, this paper only establishes a one-fourth model, which requires symmetrical boundary conditions. The mesh parameters for specimen with different porosities are shown in Table 4.

Tab. 4 - Parameter of the finite element model for specimen

Pore diameter mm	Theoretical porosity (%)	Real porosity (%)	Simulation porosity (%)	Size of the cell (mm)	Bore number	Unit number
5	10	9.5	9.5	8.7656×8.7656×8.7656	196	84672
	20	19.3	19.7	7.000×6.8930×6.8930	405	88290
	30	27.8	29.2	5.9033×6.1667×6.1667	600	76800
	40	38.7	38.5	5.700×5.4624×5.4624	792	101376

RESULTS OF THE NUMERICAL CALCULATION

The transmission wave of the incident stress wave $T_{40}F_5$

The transmission stress wave, through pressure bar 1 and SAP concrete specimens with porosity 10%, 20%, 30% and 40% respectively, of the incident stress wave $T_{40}F_5$ with pulse time 40μs and peak stress 5Mpa is shown in Figure 4.

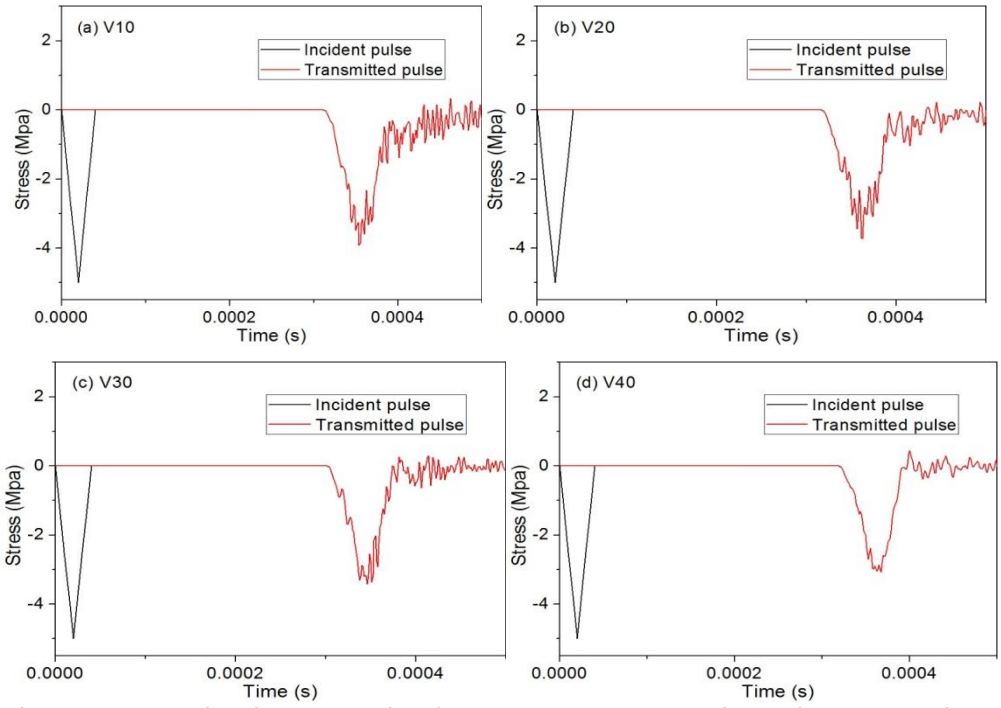

Fig. 4 – Transmitted stress pulse for stress wave $T_{40}F_5$ through pressure bar1

The transmission wave of the incident stress wave $T_{40}F_{15}$

The transmission stress wave, through pressure bar 2 and SAP concrete specimens with porosity 10%, 20%, 30% and 40% respectively, of the incident stress wave $T_{40}F_{15}$ with pulse time 40μs and peak stress 15 MPa is shown in Figure 5.

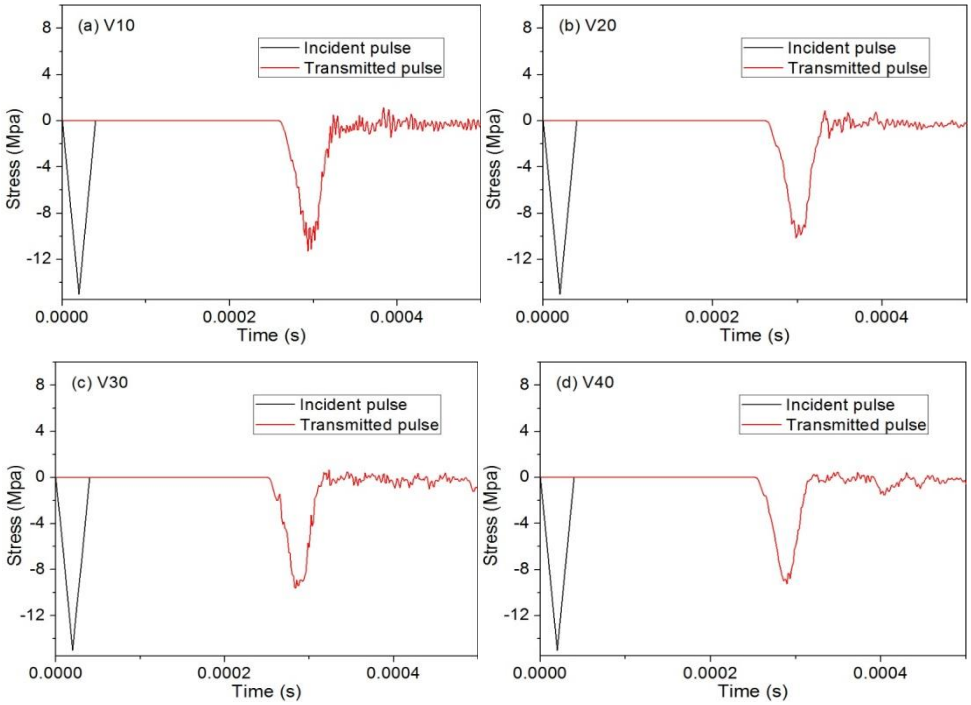

Fig. 5 – Transmitted stress pulse for stress wave $T_{40}F_{15}$ through pressure bar2

The transmission wave of the incident stress wave $T_{40}F_{25}$

The transmission stress wave, through pressure bar 1 and SAP concrete specimens with porosity 10%, 20%, 30% and 40% respectively, of the incident stress wave $T_{40}F_{25}$ with pulse time 40μs and peak stress 25 MPa is shown in Figure 6.

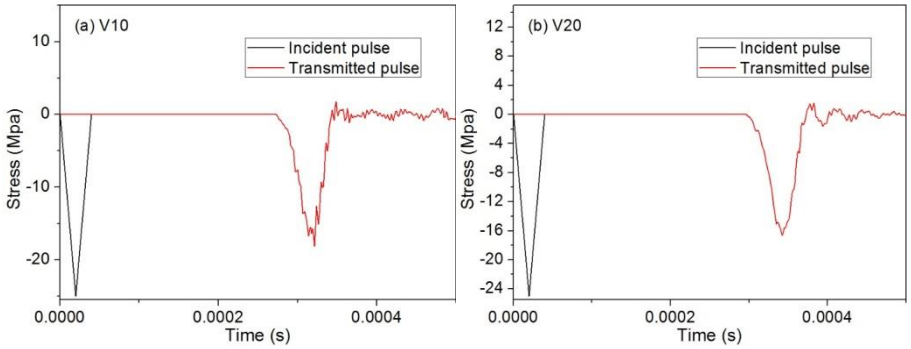

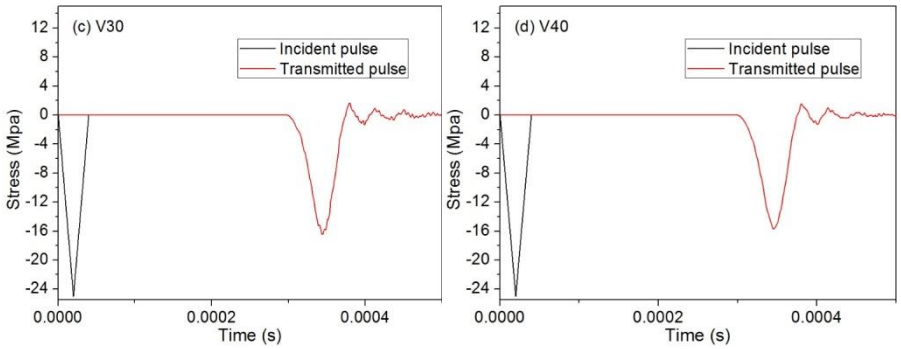

Fig. 6 – Transmitted stress pulse for stress wave $T_{40}F_{25}$ through pressure bar1

The transmission wave of the incident stress wave $T_{80}F_5$

The transmission stress wave, through pressure bar 1 and SAP concrete specimens with porosity 10%, 20%, 30% and 40% respectively, of the incident stress wave $T_{80}F_5$ with pulse time 80μs and peak stress 5 MPa is shown in Figure 7.

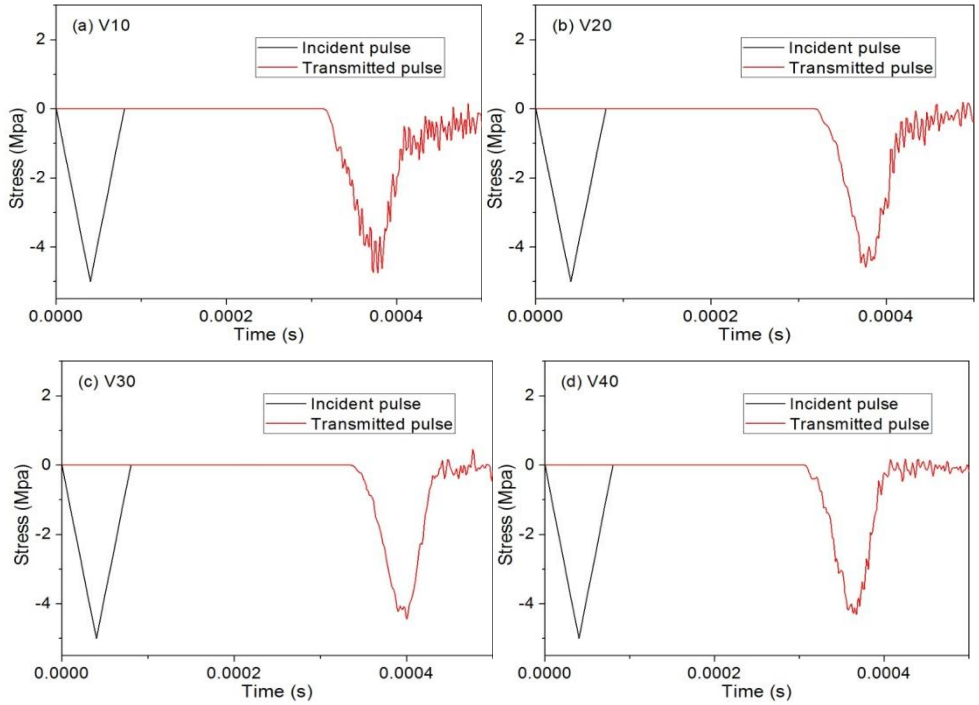

Fig. 7 – Transmitted stress pulse for stress wave $T_{80}F_5$ through pressure bar1

The transmission wave of the incident stress wave $T_{80}F_{15}$

The transmission stress wave, through pressure bar 3 and SAP concrete specimens with porosity 10%, 20%, 30% and 40% respectively, of the incident stress wave $T_{80}F_{15}$ with pulse time 80μs and peak stress 15 MPa is shown in Figure 8.

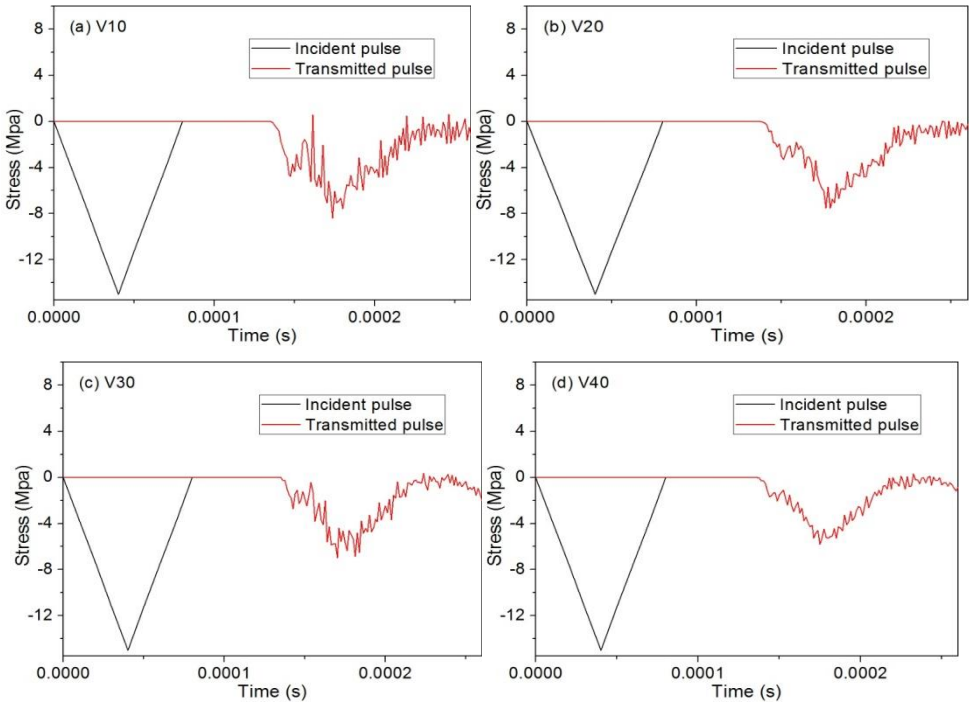

Fig. 8 – Transmitted stress pulse for stress wave $T_{80}F_{15}$ through pressure bar3

The transmission wave of the incident stress wave $T_{80}F_{25}$

The transmission stress wave, through pressure bar 1 and SAP concrete specimens with porosity 10%, 20%, 30% and 40% respectively, of the incident stress wave $T_{80}F_{25}$ with pulse time 80μs and peak stress 25 MPa is shown in Figure 9.

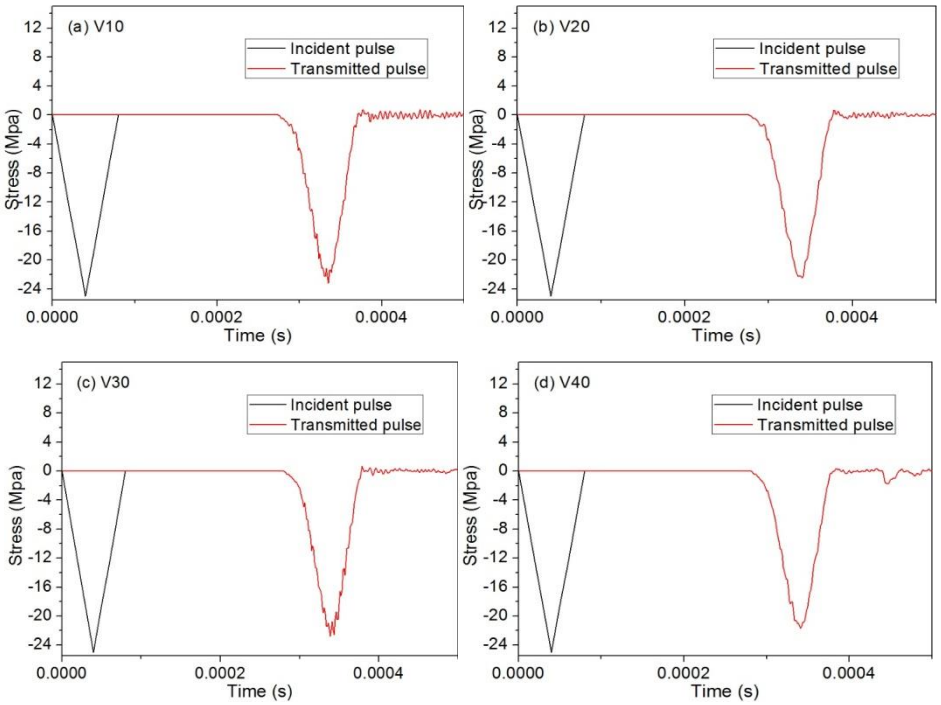

Fig. 9 – Transmitted stress pulse for stress wave $T_{80}F_{25}$ through pressure bar1

DISCUSSION

The influence of porosity on ratio of transmitted peak stress

Figure 10 shows the ratio of peak stress of transmitted stress wave and incident stress wave (ratio of transmitted peak stress) through pressure bar 1, bar 2 and bar 3 respectively with the change of porosities of specimens. In Figure 10(a) is shown the influence of SAP concrete on stress wave propagation without the influence of impedance matching of different medium. It can be seen from the Figure 10 (a) that: the ratios of transmitted peak stress are all less than 1; the ratios of transmitted peak stress decreases with increase of porosity; the ratios of transmitted peak stress of the incident stress with short pulse time is significantly smaller than that of the incident stress with long pulse time. The SAP concrete has significant attenuation for stress wave, and the attenuation will increase with rise of porosity, while decrease with increase of pulse time. Figure 10 (b) and Figure 10 (c) display the effect of SAP concrete and interface of pressure bar and specimen on propagation property of stress waves considering the impedance mismatch. It can be seen from Figure 10 (b) and Figure 10 (c) that the ratio of transmitted peak stress still increases with the rise of porosity and decrease of pulse time when there exists impedance mismatch.

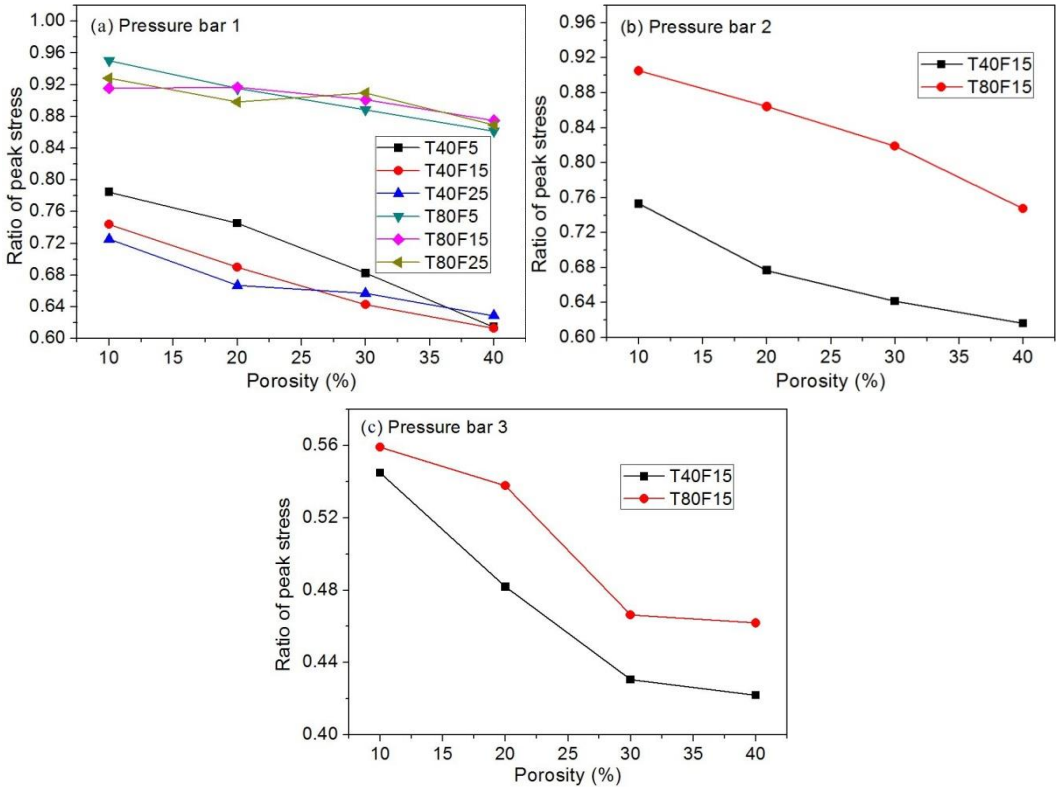

Fig. 10 – Ratio of transmitted peak stress through pressure bar 1, bar 2 and bar 3 respectively

The influence of wave impedance ratio on ratio of transmitted peak stress

Figure11 shows that the ratios of transmitted peak stress vary with porosity when incident stress wave $T_{40}F_{15}$ and $T_{80}F_{15}$propagates into specimen through pressure bar 1, pressure bar 2 and pressure bar 3 respectively. The interface impedance ratio of stress wave λ is 1, 1.56 and 5.38 on the interface of specimen and pressure bar 1, pressure bar 2 and pressure bar 3 respectively.

In Figure11 (a) and Figure 11 (b), it can be seen that the ratios of transmitted peak stress decreases with increase of the interface impedance ratio of stress wave λ, especially for the incident stress wave $T_{80}F_{15}$ with long pulse time the trend is more obvious. The ratio of transmitted peak stress is less than 0.61 and 0.88 for incident stress wave $T_{40}F_{15}$ and $T_{80}F_{15}$ respectively when the interface impedance ratio of stress wave λ is equal to 1. When the interface impedance ratio of stress wave λ rises to 5.38, the ratio of transmitted peak stress is less than o.42 and 0.46 for incident stress wave $T_{40}F_{15}$ and $T_{80}F_{15}$ respectively. The multilayer materials with SAP concrete as middle layer can greatly improve the attenuation effect of stress wave combined with attenuation effect by SAP concrete itself and adjustment of wave impedance ratio of different materials.

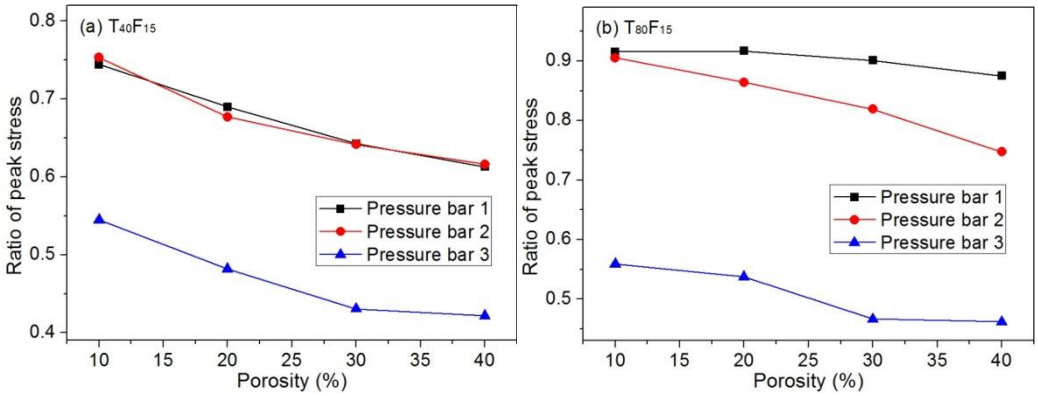

Fig. 11 – Ratio of transmitted peak stress of $T_{40}F_{15}$ and $T_{80}F_{15}$ through pressure bar 1, bar, bar 3

The dispersion effect of SAP concrete on the stress wave

As can be seen from Figure 4 to Figure 9, almost all the waveform appear dispersion phenomenon after passing through SAP concrete specimens. The wave dispersion effect includes three aspects: one is that the sharp corners of the triangle wave become smooth and even flat; the second is the rise time of stress waves will be extended; the third effect is that the stress wave oscillates after passing through SAP concrete specimens. The SAP concrete has a large number of free surface of spherical pore. Plastic stress waves can be reflected constantly between the interface and the elastic unloading wave has unloading effect. Thus, multiple steps will occur for the steep loading wave and time history curve of transmitted stress wave will appear obvious dispersion phenomenon because of step wave surface, namely the SAP concrete has significant interface dispersion effect for stress waves.

CONCLUSION

SAP concrete has attenuation function on stress waves. The SAP concrete with higher porosity has greater attenuation effect of stress wave. The attenuation effect will increase with decrease of pulse time of stress wave when given certain porosity for the concrete .The ratio of transmitted peak stress decreases with increase of the interface impedance ratio. The multilayer materials with SAP concrete as middle layer can greatly improve the attenuation effect of stress wave combined with attenuation effect by SAP concrete itself and adjustment of wave impedance ratio of different materials. SAP concrete can cause significant dispersion of stress waves, and the wave dispersion effect includes three aspects: waveform become flat; prolong the rising time; waveform oscillates after passing through SAP concrete specimens. The first two dispersion phenomenon can be attributed to the constitutive dispersion, and the third dispersion phenomenon

can be attributed to the interface diffusion. SAP concrete has significant interface dispersion effect for stress waves. Due to the lightweight in nature, energy absorbing and shock attenuation properties of the cellular concrete, which have been investigated in this research, the SAP concrete can be used in road sub-base, airport stopping pads, wall panels and composite sandwich panels.

ACKNOWLEDGEMENTS

We are indebted to the Chinese Natural Science Foundation Project of CQ CSTC (cstc2014jcyjA50026) and the Graduate Student Innovation Fund of Chongqing (CYB16127) for support of this research.

REFERENCES

[1] Wang F.Z., Yang J., Cheng H., Wu J., Liang X.Y., 2015. Study on the mechanism of desorption behavior of saturated SAP in concrete. ACI matererials journal, vol. 112: 463-470

[2] Yang J., Wang F.Z., Liu Y.P., 2015. Comparison of ordinary pores with internal cured pores produced by superabsorbent polymers. Advanced materials research, 1129: 315-322

[3] Wang F.Z., Yang J., Hu S.G., Li X.P., Cheng H., 2016. Influence of superabsorbent polymers on the surrounding cement paste. Cement and concrete research, vol. 81: 112-121

[4] Wang L., Wang Y.G., 2005. The important role of stress waves in the study on dynamic constitutive behavior of materials by SHPB. Explosion and shock waves, vol. 25: 17-25

[5] Godin O.A., Chapman D.M., 2001. Dispersion of interface waves in sediments with power-law shear speed profiles. I. Exact and approximate analytical results. Journal of the Acoustical society of america, vol. 110:1890-907

[6] Chapman D.M.F., Godin O.A., 2001. Dispersion of interface waves in sediments with power-law shear speed profiles. II. Experimental observations and seismo-acoustic inversions. Journal of the acoustical society of america,vol. 110:1908-16

[7] Murty G.S., 1975. A theoretical model for the attenuation and dispersion of stoneley waves at the loosely bonded interface of elastic half spaces. Physics of the earth & planetary interiors, vol. 11: 65-79

[8] Deng Z.P., Cheng H., Wang Z.G., Zhu G.H., Zhong H.S., 2016. Compressive behavior of the cellular concrete utilizing millimeter-size saturated SAP under high strain-rate loading. Construction and building materials, vol. 119: 96-106

[9] Deng Z.P., Cheng H., Zhu G.H., 2015. Dynamic behavior and constitutive model of super absorbent polymer concrete under impact loading. International journal of earth sciences and engineering, vol. 8: 2974-2980

[10] Drucker D.C., Prager W., 1952. Soil mechanics and plastic analysis or limit design. Quarterly of applied mathematics, vol.10: 157-165

[11] Li Q.M., Meng H., 2003. About the dynamic strength enhancement of concrete-like materials in a split Hopkinson pressure bar test . Solids and structures, vol. 40: 343-360

[12] Bischoff P.H., Perry S.H., 1991. Compressive behavior of concrete at high strain rate. Materials and structures, vol. 24: 42-450